Flexible navigation with neuromodulated cognitive maps

1 Introduction

Survival in complex environments demands efficient navigational strategies. From desert ants to humans, successful wayfinding—navigating toward goals out of sight—relies on internal spatial representations, or *cognitive maps* [1, 2]. These maps enable flexible planning and decision-making beyond simple stimulus-response associations.

Cognitive map theories propose multiple strategies for spatial navigation, ranging from simple route learning to survey-based and graph-based models. Route learning stores paths as action-position pairs but struggles with scalability and generalization at intersections [3, 4, 5]. Survey maps, grounded in Euclidean geometry, offer greater flexibility [4, 6] but sometimes contradict neural and behavioral data showing geometric distortions and topological biases [7, 8, 9, 10]. Labeled graphs strike a balance—encoding landmarks and transitions in a topological network that supports vector-like operations, planning, and prediction [11, 12, 13].

Neural substrates of spatial representations reside in the hippocampus (HP) and entorhinal cortex (EC), where specialized cells—including grid, border, speed, and place cells—encode geometric and contextual variables [14, 15, 16]. Place cells, particularly in CA1, anchor cognitive maps [17], integrating converging inputs from grid cells, CA3, and lateral EC [18, 19, 20, 21].

Neuromodulation plays a critical role in shaping this circuitry. Dopamine and other modulators adjust synaptic strength, tune place fields, and encode novelty and reward-prediction errors [22, 23, 24]. These projections reshape spatial tuning [25, 26, 27, 28], support novelty detection [23], and transmit prediction errors, particularly via lateral EC inputs [29, 30]. These mechanisms echo principles of reinforcement learning (RL), highlighting the role of neuromodulation in adapting spatial representations to behavioral relevance [31, 24].

Computational models have captured individual components of this system. Early work proposed that the hippocampus encodes spatial position and direction [32], while topological models based on route learning highlight scalability challenges [5]. More recent approaches draw from predictive coding and reinforcement learning, including successor representations and the Tolman-Eichenbaum Machine, which generalize across spatial and relational tasks while

mimicking biological activity patterns [33, 34, 35]. Path integration models trained on motion cues give rise to grid- and place-like tunings [36, 37, 38]. Others incorporate reward-driven Hebbian plasticity modulated by neuromodulators [39]. Yet, few architectures unify these ingredients into a biologically grounded system that learns online and adapts flexibly to novelty.

In this work, we introduce a biologically inspired model of cognitive map formation that integrates place cell representations, neuromodulatory signals, and graph-based spatial reasoning. The model constructs a topological map online, linking place cells along experienced trajectories and enriching them with scalar-valued modulatory signals. These modulators form analog fields across the map [40], drive local Hebbian plasticity in response to sensory prediction errors [41, 31, 42], and help maintain and adapt reward-based neural representations [43, 44, 45, 46, 34].

This architecture supports efficient goal-directed navigation without extensive offline training, leveraging spatial priors, online plasticity, and modulatory feedback. We demonstrate how this system adapts to environmental changes and how neuromodulation influences place field allocation and remapping [47, 48], linking cognitive flexibility to underlying physiological mechanisms.

The remainder of the paper is organized as follows: Section 2 details the model and experimental setup; Section 3 presents results; Section 4 discusses broader implications and future directions.

2 Methods

Our model focuses on cognitive map formation through an agent's experiences within a closed environment, as illustrated in Figure 1**a**..

The architecture operates with minimal external information—just binary reward and collision signals. Instead, spatial representation emerges primarily from idiothetic information: the agent's perception of self-motion [49]. Specifically, we use the factual velocity vector (the agent's actual environmental displacement) as the primary navigational cue, which in biological systems emerges from integrated inertial and relative motion signals [50, 51].

Place Cell Formation Spatial representation begins with a stack of grid cell modules, each encoding a periodic tiling of space over a 2D torus $\mathbf{T}^2$ (Fig.1**b,c**). Grid cell activity vectors $\mathbf{u}^{\mathrm{GC}}$ project to two place cell layers with initially zeroed weights. When no place cells activate for the current input, a silent neuron is randomly selected and imprinted with the current activity. To ensure selectivity, imprinting is aborted if the new weight vector overlaps too strongly (via cosine similarity) with existing ones.

Each place cell's activation is given by a bounded activation function based on cosine similarity. Details of lateral inhibition and recurrent connectivity are given in Appendix A.1.

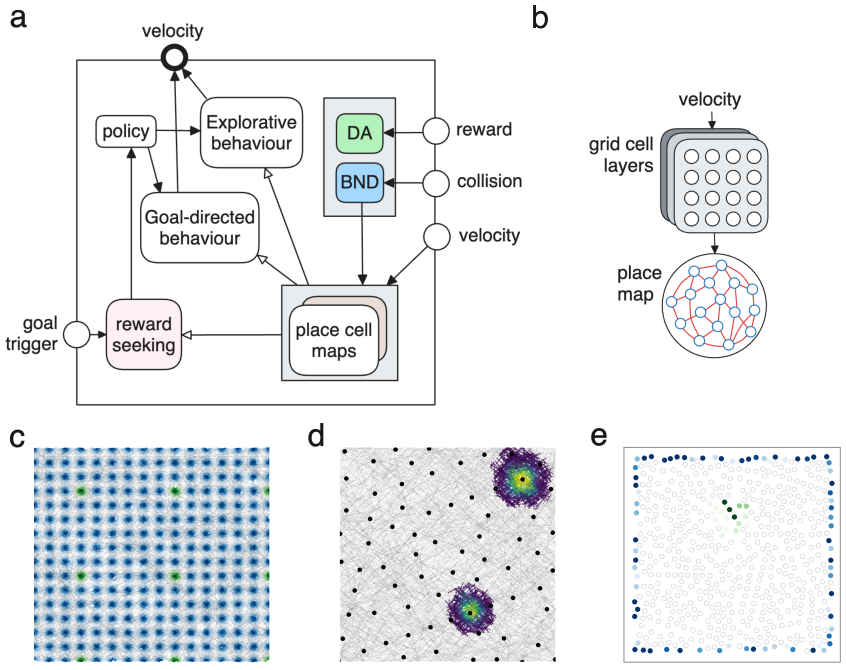

Figure 1: Model layout and spatial representations - **a**: *the full architecture of the model, consisting of three main sensory input, targeting the two modulators and the cognitive map module, and the executive components, represented by a policy module, two behavioral programs and a reward receiver.* **b**: *the cognitive map component, organized with a stack of grid cell modules receiving the velocity input and projecting to the layer of place cells.* **c**: *the neural activity of a grid cell module from a random trajectory; in blue the repeating activity of all cell, while in green the activity of only one, highlighting the periodicity in space.* **d**: *the distribution in space of the place cells centers, together with the activity of two cells showing the size of their place field.* **e**: *neuromodulation activity over the place cells map, with in blue the cells tagged by the collision modulation, and in green the ones targeted by reward modulation.*

Neuromodulation Neuromodulators encode environmental salience. Two scalar modulators, one for reward (DA) and one for boundary collisions (BND), are driven by binary inputs I and accumulate over time via exponential decay.

Each modulator k updates synaptic weights to place cells through Hebbian plasticity:

$$\Delta \mathbf{W}^{\mathrm{k}} = \eta^{\mathrm{k}} \mathrm{v}^{\mathrm{k}} \mathbf{u}^{\mathrm{PC}}$$

Weight vectors are constrained to remain non-negative. Reward modulation tags cells near rewarded locations, while boundary modulation builds a representation of environmental edges. These scalar fields form the core of the cognitive

map (Fig. 1**e**). See Appendix A.2 for full learning rules and parameter settings.

Online Adaptation To remain resilient to environmental changes (e.g., moving rewards), the model uses a predictive mechanism to correct outdated internal representations. Before executing a movement toward position $\mathbf{x}_{t+1}$, the system predicts the expected value $\hat{v}^k$ of neuromodulator k at that location. Then, a prediction error is computed and used to adjust the weights:

$$\Delta \mathbf{W}^k \leftarrow \Delta \mathbf{W}^k + \hat{\eta}^k (\hat{v}^k - v^k) \mathbf{u}^{PC}$$

The prediction learning rate $\hat{\eta}^k < 1$ ensures that small errors are corrected gradually, while repeated mismatches lead to weight depression. This mechanism implements a simple form of predictive coding and is inspired by temporal-difference learning [52], aligning with evidence that neuromodulatory systems signal prediction errors and update beliefs [53, 34, 54].

Modulation of Place Fields
We further tested whether neuromodulators could directly alter spatial tuning. Place fields were dynamically shifted and resized based on recent salience signals.

Following a salient event (reward or collision), place field centers were displaced in grid cell space, with magnitude scaled by the neuromodulator v^k and proximity to the event:

$$\Delta \mathbf{W}_i^{GC,PC} = c^k v^k \varphi_{\sigma^k}(\mathbf{u}^{GC} - \mathbf{W}_i^{GC,PC})$$

Here, φ_σ is a Gaussian function, and c^k a scaling factor. This rule is inspired by BTSP plasticity [27, 47], which shifts CA1 place fields following salient experiences. Lateral inhibition prevents field overlap during remapping.

In addition to dislocation, field size was modulated by scaling the gain of recently active neurons. The gain β_i of each cell was adjusted via a trace variable m_i. This provides a mechanism for neuromodulators to transiently enhance or suppress spatial sensitivity.

Policy and Behavior To evaluate the model's utility in navigation, we implemented a simple policy toggling between exploration and goal-seeking behavior, depending on an external goal flag and the internal map.

Exploration consisted of a stochastic walk with persistence, plus periodic plans to visit random known locations to avoid stagnation. Goal-directed navigation was triggered when a reward representation was present and executed via shortest-path planning on the place cell graph.

The graph was defined by place cells as nodes and synaptic links as edges. The agent selected targets either randomly or based on cells with high dopaminergic weight, echoing hippocampal replay and value-based navigation [55, 56, 57]. Planning was achieved via Dijkstra's algorithm with a cost function that penalized proximity to boundaries.

Table 1: Comparison of neural network models for spatial navigation and representation

Model	**Architecture**	**Training Method**	**Ext. C.**
Banino et al. [36]	LSTM + linear layers + CNN	BPTT and deep RL, supervised	Yes
Cueva et al. [38]	RNN + linear layers	Hessian-free algorithm with regularization	Yes
Sorcher et al. [37]	RNN + linear layers	Backpropagation with regularization	Yes
Whittington et al. [35]	Attractor network and deep networks	Backpropagation and Hebbian learning	No
de-Cothi et al. [34]	Successor representation	TD-learning + eligibility traces	Yes
Brozsko et al. [58]	Spike Response Model	Online modulated Hebbian plasticity	Yes
Ours	Rate layers	Online neuromodulated plasticity	No

Model	**Task**	**Input**	**Output**
Banino et al.	Path integration, goal navigation	Velocity, visual input, reward	PC, HDC
Cueva et al.	Path integration	Velocity	Position
Sorcher et al.	Path integration	Velocity	PC
Whittington et al.	Relational graph knowledge	Observation and action	Observation
de-Cothi et al.	Planned navigation	Observation	–
Brozsko et al.	Goal navigation	Position, reward	Action
Ours	Goal navigation	Velocity, reward, collision	Action

Note: PC = Place Cells, HDC = Head Direction Cells, Ext. C. = External Spatial Coordinates

Comparison with previous architectures Several previous computational models show structural and conceptual similarities with the present work. A prominent category among them employs deep neural networks—often with recurrent components—and relies on gradient-based learning strategies such as backpropagation through time. These models typically require multiple train-

ing episodes or large datasets for convergence. In contrast, our model adopts biologically inspired, synaptically local plasticity rules, and requires only a single training episode for adaptation.

Other models utilize spiking neurons [58] or explicit neural representations [34], and incorporate online learning rules more closely aligned with ours. These models also focus more directly on goal-directed navigation, in contrast to purely path integration tasks. However, both of these rely on external spatial coordinates to represent current position. Our model instead constructs an internal coordinate system by integrating its own velocity output, enabling endogenous spatial tracking.

Naturalistic task The model was evaluated on a biologically inspired navigation benchmark involving exploration and goal-seeking behavior in closed environments. Performance was measured as the total number of rewards collected over multiple trials.

3 Results

3.1 Performance in wayfinding

Our primary aim was to evaluate the formation of the cognitive map through neuromodulation in terms of the performance of the goal navigation in different environments. The best model resulting from evolution reached solid navigation and adaptation skills. The agent was able to visit a significant portion of the environment during exploration and use neuromodulation to produce useful spatial representations.

The left panel of plot 2**a** displays place cells associated with collisions and reward events, signaling boundaries (in blue) and reward (in green) locations. The overlap of these two representations and the place cells (in pink) is what we refer to as a cognitive map, since these are the main sources of spatial and contextual information used during planned navigation, whose path is depicted as a gray line. The right panel instead portrays the actual environment with walls (black), reward location (green), and multiple trajectories (red). During exploration, the main areas were visited until the reward position was located and the goal-directed navigation dominated, as highlighted by the density of the path lines. Considering the position of the walls and corners, the layout of this environment does not always make the target locations visible, as it is a non-convex area and therefore can be classified as wayfinding [59]. The challenge of not being able to use straight lines is overcome by the graph approach using local data and the consideration of boundary place cells, allowing the agent to plan accordingly. In addition, by construction the path also minimized the length of the path, within the part of the space covered by the cognitive map.

In general, this result confirms the ability of the model to focus on navigation and obstacle avoidance. However, it is worth nothing that not all simulations

resulted in a reward being found in the first place, due to the randomness of the exploratory process; this was more pronounced in complex environment.

3.1.1 Detour task

The planning ability and the plastic nature of the cognitive map should provide resilience against unexpected changes in the environment layout. In order to verify this we implemented a detour experiment. Initially, the agent was familiarized with a square environment with the reward in the middle and starting always from the same position. Then, a wall was placed in between the starting position and the reward, therefore forrcing new trajectory for reaching it. As expected, the agent was able to form a representation of the new obstacle and calculating new paths around it, succeeding the task. In plot 2**b** they are shown the trajectories before and after the wall placement, and it is manifesed the ability of detour in the new layout.

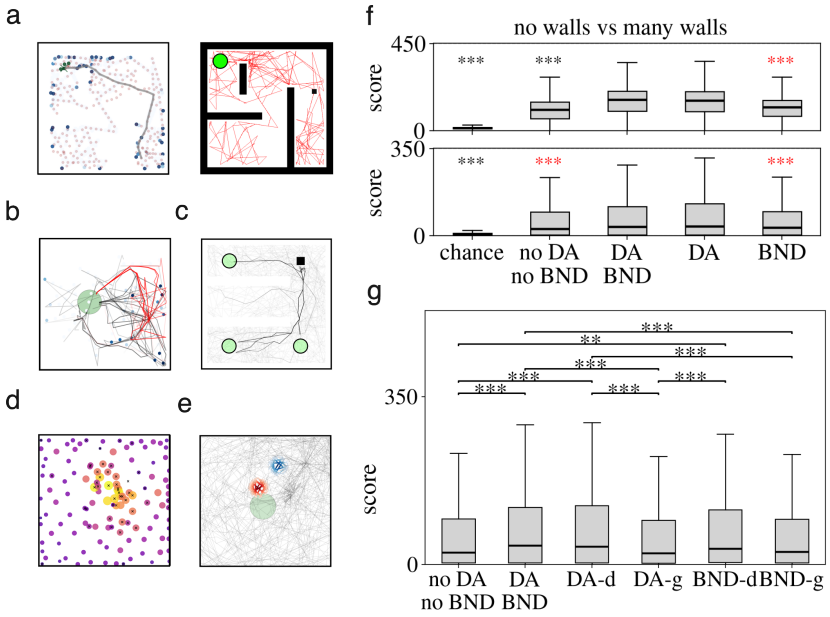

Figure 2: COGNITIVE MAPS AND PERFORMANCE RESULTS - **a**: *the plot on the left represent a cognitive map over a space, together with the plan (grey line) to reach a target location from a starting position. The plot on the right is a view of the same enviroment but with highlighted walls (black thick lines) the reward (green circle), trajectory (red line), agent position (black square).* - **b**: *plot of trajectories before (black) and after (red) the insertion of a wall between the starting and goal positions, the wall can be spotted from the boundary cells in blue* - **c**: *trajectories for multiple trials with the agent starting at the same position (black square) but with the reward location (green circles) periodically moving* - **d**: *place cells centers with size and color proportional to its node degree (number of neighbors); further, it notable is the correlation with the distance from the reward (in the center)* - **e**: *place fields of the same cell before and after several relocation of its center following reward events* - **f**: *performance comparison with same environmental conditions for five different models: one baseline as chance level (plasticity disabled, except for place cells generation), and four variants with different ablations of DA and BND modulations of place fields density and size. Results in terms of reward count and Bonferroni-corrected pairwise t-test, black stars stand for statistical difference with respect to all other groups, red starts only to the DA and DA+BND.* - **g**: *ablation performance comparison similar to* c, *and over the same environment for model variants with different active modulatory mechanisms: no DA and BND place field modulation, full DA and BND, DA-d for PC density, DA-g activation gain, BND-d for PC density,BND-g for activation gain.*

3.2 Adaptive goal representation through prediction error

Then, we tested the adaptability to environmental changes. In this scenario, the reward object was moved after being fetched a fixed number of times. Here, the difficulty was to unlearning previous locations and discovering new ones, in a protocol similar to [39]. In plot **2c** is reported the set of trajectories over many trials with the reward displaced in three possible locations. The agent was capable of planning behavior, as earlier, but also exploring and finding the new rewards, as shown by the density of lines. Whenever a goal path resulted in a failed prediction, the DA-based sensory error weakened the association between the place cells and the reward signal, leading to an extinction of its representation at that location.

This result validates the resilience of the model to changing sensory expectations, in this case the reward position.

3.3 Modulation of spatial resolution affects performance

Lastly, we investigated the effect of modulating the density of place cells and the size of the field. The goal position was fixed, but the agent was randomly relocated after fetching; performance was defined as the total number of reward counts within a time window.

Our working hypothesis is that these experience-driven neuronal changes would improve the quality of the cognitive map and be reflected in navigational abilities. The assessment of this claim was conducted by comparing variants of the model, obtained by progressively ablating the reward (DA) and collision (BND) modulation of density and field size, but a cognitive map was still possible as their representations of goals and boundaries were preserved. We also defined a chance level by instead blocking all modulation-based plasticity and allowing only place cells to form. All models were run in two different environments differing by number of internal walls, in total 2048 simulations were done for each case.

Plot **2d** showcases the distribution of place cells with the circle size and color represent the node degree, which aligns discretely with the reward position and the density. Further, in plot **2e** the place field of one cell is shown, before and after several reward occurences and consequent center relocation.

The statistical results are shown in plot **2f**. The top reports the scores in the setting without internal walls. All models performed above chance, but the main finding is the affirmation of the importance of neuronal modulation, as revealed by the statistical difference between those endowed with it and the one not. Furthermore, possession of DA modulation resulted in a significantly higher score than BND modulation alone (red stars). In fact, in a situation with a convex region such as this, once the reward has been located, the boundary information has limited utility.

A similar pattern emerged when more internal walls were introduced, as shown by the results at the bottom. In this environment, scores were overall lower as navigation became more difficult, and the difference among groups thin-

ner, although noticeable. Here, the sole presence of the boundary modulation of place cells did not result in better performance than the baseline. This outcome highlights how the main improvements are brought by reward-driven neuronal modulation (DA).

Then, in order to enquiry which particular modulatory action was mostly relevant, we conducted a similar test on the same environment but ablating not only specific neuromodulators, but also whether they affected the place cells density or the activation gain parameter. In plot 2**g** are reported the comparions among different variants. The general trend matched the previous results 2**c**, in that DA is the best neuromodulator in terms of correlation with performance. The additional finding was that density modulation is significantly the primary action behind the behavioural improvements, and alone does not perform worse that the model with all actions together.

Taken together, these findings support the hypothesis of practical utility of direct modulation of place-field structure for active navigation, even in these simple settings.

4 Discussion

Exploration and planning in known and past environment are essential behaviors of animals, directly affecting their success in world understanding and goal reaching.

An important element behind these abilities is the formation of a map of their surroundings as they make new experiences, known as a cognitive map. Numerous speculations have been made about the shape and neural foundations of such an object, varying in the types of modeling assumptions and experimental support.

The contribution of the present work was to propose a rate network model, inspired by the CA1 hippocampal region [17]. We used grid cells together with synaptic plasticity as a mechanism to develop information-rich representations based on place cells updated through experience, grouped with common perspectives on cognitive maps [60]. In the spirit of minimizing the geometric assumptions in the neural space, we treated the generated place network as a topological graph, with sensory information added locally through the action of neuromodulators. This idea aligned with the concept of a *labeled graph* [61, 8], however, it is also true that no metric violations were actually possible in these settings.

The tasks we applied the agent consisted of an exploratory and exploratory phase, in which it was prompted to plan and reach reward positions. For simplicity, the first stage relied on a random walk process, as it was outside the scope of this work. This choice had the side effect that the reward was not always discovered, leading to the formation of incomplete maps, and thus impairing performance. However, this issue was limited in frequency.

The simulation results validated the model, showing the expected emergence of cognitive maps and their encoding of information collected during the experi-

ence. The online nature of the formation of the locations on the map aligns with the idea of using only idiothetic velocity input, as in path integration [6, 62, 63]. Previous work followed a similar direction using recurrent networks, but required extensive gradient-based training [64, 38, 51]. Another important difference is that our resulting neural network was composed solely of place cells, although neuromodulated, and no other types of neuron were present. This distinction is justified by the partially different task structure, which did not involve supervised learning and did not receive visual information as in [36]. Furthermore, our model relied on predefined grid cells layers, which constituted a strong and sufficient inductive bias, and did not have to be learned from scratch.

An additional relevant aspect is also the consideration of the place cell layer as an explicit graph data structure, on which the path-planning and decision-making algorithm was applied. The adoption of this level of description lead to robustness and flexibility, enabling effective navigation in all tested environments, which varying in layout complexity. Nevertheless, this approach did act as another clear inductive bias, which lifted the need to learn an approximation of it through network dynamics and even more differently tuned neurons.

Adaptability was tested by occasionally moving the reward position, leading to the generation of an internal prediction error that was used to update its representation on the map. The agent was proved capable of unlearning previous associations, returning to exploration, and memorizing new reward locations. This behavioral protocol is similar to previous work [58], in which dopaminergic and cholinergic activity was utilized within a Hebbian plasticity rule to strengthen or weaken reward-associated spatial representations. However, alternatively to exploiting neuromodulators with opposite valence, we followed a preditive coding framework, a direction linked to hippocampal representations [34, 65] and explored various computational approaches [66, 67, 68]. This choice departed from our focus on using operations on the cognitive map itself by simulating future sensory experiences and learning from feedback. In fact, neuromodulation has been long associated with this functionality [40], especially dopamine [25, 43, 46, 31].

Lastly, the hypothesis of relevance of the active modulation of the neuronal properties of place cells was corroborated by simulating ablation experiments. These tests reported a significant impact of altering the place cells density on the total count of collected rewards. In general, these results are consistent with the experimental observations of alteration of place cells following reward events [27, 69], in particular in terms of increased clustering of cells [70, 71], reminiscent of changes in firing rate after contextual changes [72, 73].

Concerning the modulation of place fields, there is significant experimental evidence of their alternation during reward events [74, 75, 76], some reporting shrinkage near reward objects [77], and boundaries [78]. The coupling with higher local density could be explained by better optimization of the cell distribution for goal representation and planning [79]. However, in our settings, the fields become enlarged, especially in the direction of the target, although the performance improvements were not tested significant. A possible explanation can be the simplicity of our reward, which was solely defined as an area of space.

The lack of rich non-spatial features thus did not require the place cells to code for smaller spatial variation. Therefore, enlargement might have improved the stability of the representation, marking the nodes associated with rewards more solidly, given the stochasticity of its delivery. Further, the graph-path algorithm utilized the strength of the DA-modulated connections for determining the goal representation, stronger fields inherently developed stronger weights, making planning more reliable planning. Although these findings are limited within the limit of our simulation protocol, there have been experimental observations of elongation of place fields along trajectories over meaningful experiences [80, 81].

In conclusion, this work showed a possible architecture for coupling emergent spatial representations with neuromodulated plasticity to achieve an experience-driven cognitive map. The reliance of few spatial and algorithmic inductive biases, grid cells and planning algorithm, supports the idea of label graph for goal navigation. Future work can investigate the application to other spatial domains, such as motor control and three-dimensional navigation. In addition, a richer input feature can be added, such as visual information [82], as well as new neuromodulators that encode different sensory dimensions or internally generated signals.

Acknowledgements & Statements
The authors declare no competing interests.
The code is publicly available and can be found at `https://github.com/iKiru-hub/PCNN`.
This research was funded by the European Union's Horizon 2020 research and innovation programme under the Marie Skłodowska-Curie grant agreement Nº 945371 and the University of Oslo.
The research presented in this paper has benefited from the Experimental Infrastructure for Exploration of Exascale Computing (eX3), which is financially supported by the Research Council of Norway under contract 270053.

References

[1] Reginald Golledge, Dan Jacobson, Rob Kitchin, and Mark Blades. Cognitive Maps, Spatial Abilities, and Human Wayfinding. *GEOGRAPHICAL REVIEW OF JAPAN SERIES B*, 73:93–104, December 2000.

[2] Russell A. Epstein and Lindsay K. Vass. Neural systems for landmark-based wayfinding in humans. *Philosophical Transactions of the Royal Society B: Biological Sciences*, 369(1635):20120533, February 2014.

[3] Michael Peer, Iva K. Brunec, Nora S. Newcombe, and Russell A. Epstein. Structuring Knowledge with Cognitive Maps and Cognitive Graphs. *Trends in cognitive sciences*, 25(1):37–54, January 2021.

[4] Elizabeth R. Chrastil and William H. Warren. From Cognitive Maps to Cognitive Graphs. *PLoS ONE*, 9(11):e112544, November 2014.

[5] Steffen Werner, Bernd Krieg-Brückner, and Theo Herrmann. Modelling Navigational Knowledge by Route Graphs. In Christian Freksa, Christopher Habel, Wilfried Brauer, and Karl F. Wender, editors, *Spatial Cognition II: Integrating Abstract Theories, Empirical Studies, Formal Methods, and Practical Applications*, pages 295–316. Springer, Berlin, Heidelberg, 2000.

[6] C. R. Gallistel and Audrey E. Cramer. Computations on Metric Maps in Mammals: Getting Oriented and Choosing a Multi-Destination Route. *Journal of Experimental Biology*, 199(1):211–217, January 1996.

[7] Michael Peer, Catherine Nadar, and Russell A. Epstein. The format of the cognitive map depends on the structure of the environment. *Journal of Experimental Psychology: General*, 153(1):224–240, January 2024.

[8] William H. Warren. Non-Euclidean navigation. *Journal of Experimental Biology*, 222(Suppl_1):jeb187971, February 2019.

[9] Mark Wagner. Comparing the psychophysical and geometric characteristics of spatial perception and cognitive maps. *Cognitive Studies: Bulletin of the Japanese Cognitive Science Society*, 15(1):6–21, 2008.

[10] Rainer Rothkegel, Karl F. Wender, and Sabine Schumacher. Judging Spatial Relations from Memory. In Christian Freksa, Christopher Habel, and Karl F. Wender, editors, *Spatial Cognition: An Interdisciplinary Approach to Representing and Processing Spatial Knowledge*, pages 79–105. Springer, Berlin, Heidelberg, 1998.

[11] Tobias Meilinger. The Network of Reference Frames Theory: A Synthesis of Graphs and Cognitive Maps. In Christian Freksa, Nora S. Newcombe, Peter Gärdenfors, and Stefan Wölfl, editors, *Spatial Cognition VI. Learning, Reasoning, and Talking about Space*, pages 344–360, Berlin, Heidelberg, 2008. Springer.

[12] Jane X. Wang, Zeb Kurth-Nelson, Dhruva Tirumala, Hubert Soyer, Joel Z. Leibo, Remi Munos, Charles Blundell, Dharshan Kumaran, and Matt Botvinick. Learning to reinforcement learn, January 2017.

[13] Victor R. Schinazi, Daniele Nardi, Nora S. Newcombe, Thomas F. Shipley, and Russell A. Epstein. Hippocampal size predicts rapid learning of a cognitive map in humans. *Hippocampus*, 23(6):515–528, 2013.

[14] Francesca Sargolini, Marianne Fyhn, Torkel Hafting, Bruce L. McNaughton, Menno P. Witter, May-Britt Moser, and Edvard I. Moser. Conjunctive Representation of Position, Direction, and Velocity in Entorhinal Cortex. *Science*, 312(5774):758–762, May 2006.

[15] Emilio Kropff, James E. Carmichael, May-Britt Moser, and Edvard I. Moser. Speed cells in the medial entorhinal cortex. *Nature*, 523(7561):419–424, July 2015.

[16] Trygve Solstad, Edvard I. Moser, and Gaute T. Einevoll. From grid cells to place cells: A mathematical model. *Hippocampus*, 16(12):1026–1031, 2006.

[17] Flavio Donato, Anja Xu Schwartzlose, and Renan Augusto Viana Mendes. How Do You Build a Cognitive Map? The Development of Circuits and Computations for the Representation of Space in the Brain. *Annual Review of Neuroscience*, 46(Volume 46, 2023):281–299, July 2023.

[18] Daniel Bush, Caswell Barry, and Neil Burgess. What do grid cells contribute to place cell firing? *Trends in Neurosciences*, 37(3):136–145, March 2014.

[19] Torsten Neher, Amir Hossein Azizi, and Sen Cheng. From grid cells to place cells with realistic field sizes. *PLOS ONE*, 12(7):e0181618, July 2017.

[20] Tianyi Li, Angelo Arleo, and Denis Sheynikhovich. *Modeling Place Cells and Grid Cells in Multi-Compartment Environments: Hippocampal-Entorhinal Loop as a Multisensory Integration Circuit*. April 2019.

[21] Olesia M. Bilash, Spyridon Chavlis, Cara D. Johnson, Panayiota Poirazi, and Jayeeta Basu. Lateral entorhinal cortex inputs modulate hippocampal dendritic excitability by recruiting a local disinhibitory microcircuit. *Cell Reports*, 42(1):111962, January 2023.

[22] John E. Lisman and Anthony A. Grace. The Hippocampal-VTA Loop: Controlling the Entry of Information into Long-Term Memory. *Neuron*, 46(5):703–713, June 2005.

[23] Adrian J. Duszkiewicz, Colin G. McNamara, Tomonori Takeuchi, and Lisa Genzel. Novelty and Dopaminergic Modulation of Memory Persistence: A Tale of Two Systems. *Trends in Neurosciences*, 42(2):102–114, February 2019.

[24] Wolfram Schultz, Peter Dayan, and P. Read Montague. A Neural Substrate of Prediction and Reward. *Science*, 275(5306):1593–1599, March 1997.

[25] Kimberly A. Kempadoo, Eugene V. Mosharov, Se Joon Choi, David Sulzer, and Eric R. Kandel. Dopamine release from the locus coeruleus to the dorsal hippocampus promotes spatial learning and memory. *Proceedings of the National Academy of Sciences*, 113(51):14835–14840, December 2016.

[26] Aude Retailleau and Thomas Boraud. The Michelin red guide of the brain: Role of dopamine in goal-oriented navigation. *Frontiers in Systems Neuroscience*, 8, March 2014.

[27] Katie C. Bittner, Aaron D. Milstein, Christine Grienberger, Sandro Romani, and Jeffrey C. Magee. Behavioral time scale synaptic plasticity underlies CA1 place fields. *Science*, 357(6355):1033–1036, September 2017.

[28] Alexandra Mansell Kaufman, Tristan Geiller, and Attila Losonczy. A Role for the Locus Coeruleus in Hippocampal CA1 Place Cell Reorganization during Spatial Reward Learning. *Neuron*, 105(6):1018–1026.e4, March 2020.

[29] Kei M. Igarashi, Hiroshi T. Ito, Edvard I. Moser, and May-Britt Moser. Functional diversity along the transverse axis of hippocampal area CA1. *FEBS Letters*, 588(15):2470–2476, August 2014.

[30] Hiroshi T. Ito and Erin M. Schuman. Functional division of hippocampal area CA1 via modulatory gating of entorhinal cortical inputs. *Hippocampus*, 22(2):372–387, 2012.

[31] Denis Sheynikhovich, Satoru Otani, Jing Bai, and Angelo Arleo. Long-term memory, synaptic plasticity and dopamine in rodent medial prefrontal cortex: Role in executive functions. *Frontiers in Behavioral Neuroscience*, 16, January 2023.

[32] Bruno Poucet. Spatial cognitive maps in animals: New hypotheses on their structure and neural mechanisms. *Psychological Review*, 100(2):163–182, 1993.

[33] Paul Stoewer, Achim Schilling, Andreas Maier, and Patrick Krauss. Neural network based formation of cognitive maps of semantic spaces and the putative emergence of abstract concepts. *Scientific Reports*, 13(1):3644, March 2023.

[34] William de Cothi, Nils Nyberg, Eva-Maria Griesbauer, Carole Ghanamé, Fiona Zisch, Julie M. Lefort, Lydia Fletcher, Coco Newton, Sophie Renaudineau, Daniel Bendor, Roddy Grieves, Éléonore Duvelle, Caswell Barry, and Hugo J. Spiers. Predictive maps in rats and humans for spatial navigation. *Current Biology*, 32(17):3676–3689.e5, September 2022.

[35] James C. R. Whittington, Timothy H. Muller, Shirley Mark, Guifen Chen, Caswell Barry, Neil Burgess, and Timothy E. J. Behrens. The Tolman-Eichenbaum Machine: Unifying Space and Relational Memory through Generalization in the Hippocampal Formation. *Cell*, 183(5):1249–1263.e23, November 2020.

[36] Andrea Banino, Caswell Barry, Benigno Uria, Charles Blundell, Timothy Lillicrap, Piotr Mirowski, Alexander Pritzel, Martin J. Chadwick, Thomas Degris, Joseph Modayil, Greg Wayne, Hubert Soyer, Fabio Viola, Brian Zhang, Ross Goroshin, Neil Rabinowitz, Razvan Pascanu, Charlie Beattie, Stig Petersen, Amir Sadik, Stephen Gaffney, Helen King, Koray Kavukcuoglu, Demis Hassabis, Raia Hadsell, and Dharshan Kumaran.

Vector-based navigation using grid-like representations in artificial agents. *Nature*, 557(7705):429–433, May 2018.

[37] Ben Sorscher, Gabriel Mel, Surya Ganguli, and Samuel Ocko. A unified theory for the origin of grid cells through the lens of pattern formation. In *Advances in Neural Information Processing Systems*, volume 32. Curran Associates, Inc., 2019.

[38] Christopher J. Cueva and Xue-Xin Wei. Emergence of grid-like representations by training recurrent neural networks to perform spatial localization, March 2018.

[39] Zuzanna Brzosko, Susanna B. Mierau, and Ole Paulsen. Neuromodulation of Spike-Timing-Dependent Plasticity: Past, Present, and Future. *Neuron*, 103(4):563–581, August 2019.

[40] Marielena Sosa, Mark H. Plitt, and Lisa M. Giocomo. Hippocampal sequences span experience relative to rewards. *bioRxiv*, page 2023.12.27.573490, February 2024.

[41] Abdullahi Ali, Nasir Ahmad, Elgar de Groot, Marcel A. J. van Gerven, and Tim C. Kietzmann. Predictive coding is a consequence of energy efficiency in recurrent neural networks, November 2021.

[42] Jacopo Bono, Sara Zannone, Victor Pedrosa, and Claudia Clopath. Learning predictive cognitive maps with spiking neurons during behavior and replays. *eLife*, 12:e80671, March 2023.

[43] Wolfram Schultz. Dopamine reward prediction error coding. *Dialogues in Clinical Neuroscience*, 18(1):23–32, March 2016.

[44] Jeffrey B. Inglis, Vivian V. Valentin, and F. Gregory Ashby. Modulation of Dopamine for Adaptive Learning: A Neurocomputational Model. *Computational brain & behavior*, 4(1):34–52, March 2021.

[45] Philippe N. Tobler, Christopher D. Fiorillo, and Wolfram Schultz. Adaptive Coding of Reward Value by Dopamine Neurons. *Science*, 307(5715):1642–1645, March 2005.

[46] Roshan Cools. Chemistry of the Adaptive Mind: Lessons from Dopamine. *Neuron*, 104(1):113–131, October 2019.

[47] Aaron D Milstein, Yiding Li, Katie C Bittner, Christine Grienberger, Ivan Soltesz, Jeffrey C Magee, and Sandro Romani. Bidirectional synaptic plasticity rapidly modifies hippocampal representations. *eLife*, 10:e73046, December 2021.

[48] André A. Fenton. Remapping revisited: How the hippocampus represents different spaces. *Nature Reviews Neuroscience*, 25(6):428–448, June 2024.

[49] Luxin Zhou and Yong Gu. Cortical Mechanisms of Multisensory Linear Self-motion Perception. *Neuroscience Bulletin*, 39(1):125–137, July 2022.

[50] Steven J. Jerjian, Devin R. Harsch, and Christopher R. Fetsch. Self-motion perception and sequential decision-making: Where are we heading? *Philosophical Transactions of the Royal Society B: Biological Sciences*, 378(1886):20220333, August 2023.

[51] Ian Q. Whishaw and Brian L. Brooks. Calibrating space: Exploration is important for allothetic and idiothetic navigation. *Hippocampus*, 9(6):659–667, 1999.

[52] Richard S Sutton and Andrew G Barto. The Reinforcement Learning Problem.

[53] P. R. Montague, P. Dayan, and T. J. Sejnowski. A framework for mesencephalic dopamine systems based on predictive Hebbian learning. *Journal of Neuroscience*, 16(5):1936–1947, March 1996.

[54] Seetha Krishnan, Chad Heer, Chery Cherian, and Mark E. J. Sheffield. Reward expectation extinction restructures and degrades CA1 spatial maps through loss of a dopaminergic reward proximity signal. *Nature Communications*, 13(1):6662, November 2022.

[55] Colin G. McNamara, Álvaro Tejero-Cantero, Stéphanie Trouche, Natalia Campo-Urriza, and David Dupret. Dopaminergic neurons promote hippocampal reactivation and spatial memory persistence. *Nature Neuroscience*, 17(12):1658–1660, December 2014.

[56] Frédéric Michon, Esther Krul, Jyh-Jang Sun, and Fabian Kloosterman. Single-trial dynamics of hippocampal spatial representations are modulated by reward value. *Current biology: CB*, 31(20):4423–4435.e5, October 2021.

[57] Philip Shamash and Tiago Branco. Mice identify subgoal locations through an action-driven mapping process, December 2021.

[58] Zuzanna Brzosko, Sara Zannone, Wolfram Schultz, Claudia Clopath, and Ole Paulsen. Sequential neuromodulation of Hebbian plasticity offers mechanism for effective reward-based navigation. *eLife*, 6:e27756, 2017.

[59] Tobias Meilinger, Marianne Strickrodt, and Heinrich H. Bülthoff. Qualitative differences in memory for vista and environmental spaces are caused by opaque borders, not movement or successive presentation. *Cognition*, 155:77–95, October 2016.

[60] Vincent Hok, Pierre-Pascal Lenck-Santini, Sébastien Roux, Etienne Save, Robert U. Muller, and Bruno Poucet. Goal-Related Activity in Hippocampal Place Cells. *Journal of Neuroscience*, 27(3):472–482, January 2007.

[61] Toru Ishikawa and Daniel R. Montello. Spatial knowledge acquisition from direct experience in the environment: Individual differences in the development of metric knowledge and the integration of separately learned places. *Cognitive Psychology*, 52(2):93–129, March 2006.

[62] Sabine Gillner and Hanspeter A. Mallot. Navigation and Acquisition of Spatial Knowledge in a Virtual Maze. *Journal of Cognitive Neuroscience*, 10(4):445–463, July 1998.

[63] Bruce L. McNaughton, Francesco P. Battaglia, Ole Jensen, Edvard I. Moser, and May-Britt Moser. Path integration and the neural basis of the 'cognitive map'. *Nature Reviews Neuroscience*, 7(8):663–678, August 2006.

[64] Ben Sorscher, Gabriel C. Mel, Samuel A. Ocko, Lisa M. Giocomo, and Surya Ganguli. A unified theory for the computational and mechanistic origins of grid cells. *Neuron*, 111(1):121–137.e13, January 2023.

[65] Fraser Aitken and Peter Kok. Hippocampal representations switch from errors to predictions during acquisition of predictive associations. *Nature Communications*, 13(1):3294, June 2022.

[66] Manu Srinath Halvagal and Friedemann Zenke. The combination of Hebbian and predictive plasticity learns invariant object representations in deep sensory networks. *Nature Neuroscience*, pages 1–10, October 2023.

[67] Alexander Ororbia. Spiking neural predictive coding for continually learning from data streams. *Neurocomputing*, 544:126292, August 2023.

[68] Kimberly L Stachenfeld, Matthew M Botvinick, and Samuel J Gershman. The hippocampus as a predictive map. *Nature Neuroscience*, 20(11):1643–1653, November 2017.

[69] Indrajith R. Nair, Guncha Bhasin, and Dipanjan Roy. Hippocampus Maintains a Coherent Map Under Reward Feature–Landmark Cue Conflict. *Frontiers in Neural Circuits*, 16, April 2022.

[70] Valerie L. Tryon, Marsha R. Penner, Shawn W. Heide, Hunter O. King, Joshua Larkin, and Sheri J. Y. Mizumori. Hippocampal neural activity reflects the economy of choices during goal-directed navigation. *Hippocampus*, 27(7):743–758, July 2017.

[71] Hannah S Wirtshafter and Matthew A Wilson. Differences in reward biased spatial representations in the lateral septum and hippocampus. *eLife*, 9:e55252, May 2020.

[72] Michael I. Anderson and Kathryn J. Jeffery. Heterogeneous Modulation of Place Cell Firing by Changes in Context. *Journal of Neuroscience*, 23(26):8827–8835, October 2003.

[73] Inah Lee, Amy L. Griffin, Eric A. Zilli, Howard Eichenbaum, and Michael E. Hasselmo. Gradual Translocation of Spatial Correlates of Neuronal Firing in the Hippocampus toward Prospective Reward Locations. *Neuron*, 51(5):639–650, September 2006.

[74] Marianne Fyhn, Sturla Molden, Stig Hollup, May-Britt Moser, and Edvard I. Moser. Hippocampal Neurons Responding to First-Time Dislocation of a Target Object. *Neuron*, 35(3):555–566, August 2002.

[75] P.-P. Lenck-Santini, B. Rivard, R.u. Muller, and B. Poucet. Study of CA1 place cell activity and exploratory behavior following spatial and nonspatial changes in the environment. *Hippocampus*, 15(3):356–369, 2005.

[76] David Dupret, Joseph O'Neill, Barty Pleydell-Bouverie, and Jozsef Csicsvari. The reorganization and reactivation of hippocampal maps predict spatial memory performance. *Nature Neuroscience*, 13(8):995–1002, August 2010.

[77] S.N. Burke, A.P. Maurer, S. Nematollahi, A.R. Uprety, J.L. Wallace, and C.A. Barnes. The Influence of Objects on Place Field Expression and Size in Distal Hippocampal CA1. *Hippocampus*, 21(7):783–801, July 2011.

[78] Sander Tanni, William De Cothi, and Caswell Barry. State transitions in the statistically stable place cell population correspond to rate of perceptual change. *Current Biology*, 32(16):3505–3514.e7, August 2022.

[79] Pablo Scleidorovich, Jean-Marc Fellous, and Alfredo Weitzenfeld. Adapting hippocampus multi-scale place field distributions in cluttered environments optimizes spatial navigation and learning. *Frontiers in Computational Neuroscience*, 16:1039822, December 2022.

[80] Mayank R. Mehta, Carol A. Barnes, and Bruce L. McNaughton. Experience-dependent, asymmetric expansion of hippocampal place fields. *Proceedings of the National Academy of Sciences*, 94(16):8918–8921, August 1997.

[81] Jangho Lee, Jeonghee Jo, Byounghwa Lee, Jung-Hoon Lee, and Sungroh Yoon. Brain-inspired Predictive Coding Improves the Performance of Machine Challenging Tasks. *Frontiers in Computational Neuroscience*, 16:1062678, 2022.

[82] John H. Wen, Ben Sorscher, Emily A. Aery Jones, Surya Ganguli, and Lisa M. Giocomo. One-shot entorhinal maps enable flexible navigation in novel environments. *Nature*, 635(8040):943–950, November 2024.

[83] Yuri Dabaghian. Grid Cells, Border Cells and Discrete Complex Analysis.

[84] Vemund Sigmundson Schøyen, Kosio Beshkov, Markus Borud Pettersen, Erik Hermansen, Konstantin Holzhausen, Anders Malthe-Sørenssen, Marianne Fyhn, and Mikkel Elle Lepperød. Hexagons all the way down: Grid

cells as a conformal isometric map of space. *PLOS Computational Biology*, 21(2):e1012804, February 2025.

5 Appendix

5.1 Grid cell module

Unlike other approaches to generate grid fields [83, 84], we defined a correspondence between the global environment in which the agent moves, a two-dimensional Euclidean space $\mathbf{R}^2$, and a bounded local space of a grid module, corresponding to the torus.

The global velocity $\mathbf{v} = \{\mathrm{x}, \mathrm{y}\}$ is then mapped to a local velocity, scaled by a speed scalar $\mathrm{s}_\mathrm{l}^{\mathrm{gc}}$ specific to the grid cell module l, which determines its periodicity in space. This approach has been used in previous works [20].

The choice of a toroidal space is motivated by consolidated experimental evidence of the neural space of grid cells, which are organized in modules of different sizes spanning the animal's environment. However, the shape of their firing pattern is known to be hexagonal, which corresponds to the optimal tiling of a two-dimensional plane, giving rise to a neural space lying on a twisted torus. In this work, for simplicity, we consider a square tiling and thus a square torus, without much loss of generality except for the slight increase of grid cells required for a sufficiently cover.

A grid cell module l of size N^{gc} is identified by a set of positions defined over a square centered on the origin and size of 2, such that $\{(\mathrm{x_i}, \mathrm{y_i}) \mid \mathrm{i} \in \mathrm{N}^{\mathrm{gc}} \wedge \mathrm{x_i}, \mathrm{y_i} \in (-1, 1)\}$. This local square space has boundary conditions for each dimension, such that, for instance, when $\mathrm{x_t} + \mathrm{s}_\mathrm{l}^{\mathrm{gc}} \cdot \mathrm{v_x} > 2$ the position update is taken to the other side $\mathrm{x_{t+1}} = \mathrm{x_t} + \mathrm{s}_\mathrm{l}^{\mathrm{gc}} \cdot \mathrm{v_x} - 2$, where $\mathrm{s}_\mathrm{l}^{\mathrm{gc}}$ is the scale of the velocity in the local space of the module l with respect to the real global agent velocity $\mathrm{v} = \{\mathrm{v_x}, \mathrm{v_y}\}$. When the module is initialized, the starting positions of its cells are uniformly distributed over the square forming a lattice. When the agent is reset in a new position at the beginning of new trial, a displacement vector is applied to the last cells positions such that the mapping between the module local space and the global environment is preserved.

The firing rate vector of each cell is determined with respect to a 2D Gaussian tuning curve centered at the origin at $(0, 0)$, and it is calculated as $\mathrm{r_i} = \exp\left(-\frac{\mathrm{x_i^2}+\mathrm{y_i^2}}{\sigma_\mathrm{l}^{\mathrm{gc}}}\right)$, where $\sigma_\mathrm{l}^{\mathrm{gc}}$ is the width of the tuning curve for module l.

The final population vector of the grid cell network GC is the concatenated and flattened firing rate vector of all modules $\mathbf{u}^{\mathrm{GC}}$.

In our model, each grid cell had a tuning width of 0.04. They were defined as 8 modules of size 36, and the relative speed scales were $\{1., 0.8, 0.7, 0.5, 0.4, 0.3, 0.2, 0.1, 0.07\}$.

5.2 Place cells

Tuning formation The tuning of a new place cell is simply defined as the current GC population vector $\mathbf{u}_t^{GC}$, and its index is that of the first silent cell, which is added to the forward weight matrix $\mathbf{W}_i^{GCtoPC} \leftarrow \mathbf{u}^{GC}$.

In order to avoid overlapping of place fields, the tuning process is aborted in case the cosine similarity of the new pattern and the old ones is greater than a threshold θ_{rep}^{PC}.

Each cell represents a position in the GC activity space, which can be considered a node within a graph of place cells (PC). Although it is totally possible to only use the N^{GC}-dimensional tuning patterns and be agnostic about the dimensionality of the space in which the agent lives, to simplify the calculations, we mapped each pattern to 2D positions in a vector space. Then, the PC recurrent connectivity matrix is calculated with a nearest neighbors algorithm, which instead of a fixed number K of neighbors uses a distance threshold θ_{rec}^{PC}.

Activity The current firing rate of the PC population is determined by the cosine similarity between the GC input and the forward weight matrix, then passed through a generalized sigmoid $\phi(z) = [1 + \exp(-\beta(z - \alpha))]^{-1}$. The parameter α represents the activation threshold, or horizontal offset, while β the gain, or steepness.

$$u_i^{PC} = \phi\left(\cos\left(\mathbf{u}^{GC}, \mathbf{W}_i^{GC,PC}\right)\right) \tag{1}$$

It is also defined as an activity trace, which has an upper value of 1 and decays exponentially:

$$m_i = -m_i/\tau^{PC} + u_i \tag{2}$$

It is used as a proxy for a memory trace.

In the model, a PC population is defined by its average place field size, determining the granularity of the representation of the place.

Below, a table of the parameters specific to the two PC populations is reported.

	β	α	θ_{rep}^{PC}	θ_{rec}^{PC}	τ^{PC}
pc	33.0	1.0	0.86	43	140

Table 2: PC LAYER PARAMETERS

5.3 Modulation

Neuromodulation is defined in terms of a leaky variable v whose state is perturbed by an external input x, whose qualitative meaning differs for each neuromodulator k.

$$\begin{aligned} \mathrm{v_k} &= -\mathrm{v_k}/\tau_\mathrm{k} + \mathrm{x_k} \\ \mathrm{v_k} &= \max(\mathrm{v_k}, 0) \end{aligned} \tag{3}$$

Learning rule The connection weights $\mathbf{W}^\mathrm{k}$ are updated according to a plasticity rule composed of an Hebbian term, involving the leaky variable and the place cells above a certain threshold θ^k, and a prediction error.

A prediction $\mathbf{p}$ is calculated before each time-step and signifies the expected neuromodulation activation for a given place cell $\hat{\mathrm{v}}_\mathrm{i}^\mathrm{k} = \mathbf{W}_\mathrm{i}^\mathrm{k}\hat{\mathrm{u}}_\mathrm{i}^\mathrm{PC}$, where $\hat{\mathrm{u}}_\mathrm{i}^\mathrm{PC}$ is the PC population vector obtained by simulating the planned action. A prediction error is computed as the difference between the prediction and the current modulated place activation.

The full connection update then becomes:

$$\Delta\mathbf{W}_\mathrm{i}^\mathrm{k} = \eta^\mathrm{k}\mathrm{v}^\mathrm{k}\mathrm{u}_\mathrm{i}^\mathrm{PC} - \eta_\mathrm{pred}^\mathrm{k}(\hat{\mathrm{v}}_\mathrm{i}^\mathrm{k} - \mathrm{v}_\mathrm{i}^\mathrm{k})\mathrm{u}^\mathrm{PC} \tag{4}$$

where η^k, $\eta_\mathrm{pred}^\mathrm{k}$ are the learning rates, interpretable as the weight contribution of the Hebbian coupling and prediction accuracy respectively. Additionally, connections values are kept non-negative and, in order to speed up the extinction of past place-reward associations, if a non-zero prediction error is below a 0.5 then it is set to 0.5.

Active neuronal modulation Neuromodulation acts on the neuronal profile of the place cells by affecting the value of the activation gain and relocate the center of their tuning.

Gain modulation is implemented using the activity traces and a constant reference gain value $\bar{\beta}$:

$$\beta_\mathrm{i} = \mathrm{c}_\mathrm{a}^\mathrm{k}\mathrm{m}_\mathrm{i}\bar{\beta} + (1 - \mathrm{m}_\mathrm{i})\bar{\beta} \tag{5}$$

where $\mathrm{c}_\mathrm{a}^\mathrm{k}$ is a scaling gain parameter, and if it is 1 then no modulation takes place.

Concerning center relocation, it is applied to recently active neurons with non-zero trace $\mathrm{m_i}$. For a place cell i with position $\mathbf{x}_\mathrm{i}$ (in the vector space), it is calculated a displacement vector $\mathrm{q_i}$ with respect to the current position $\mathbf{x}_\mathrm{j}$, identified as the most active place cell j.

$$\mathrm{q_i} = \mathrm{c}_\mathrm{b}^\mathrm{k}\mathrm{v}^\mathrm{k}\exp\left(-\frac{\|\mathbf{x}_\mathrm{i} - \mathbf{x}_\mathrm{j}\|}{\sigma^\mathrm{k}}\right) \tag{6}$$

where $\mathrm{c}_\mathrm{b}^\mathrm{k}$ is a scaling relocation parameter, while σ^k the width of the Gaussian distance. This displacemented is used to move in GC activity space and get the new GC population vector to use as tuning pattern.

Also in this case, it is ensured that the new place field center is at a minimum distance $\theta_\mathrm{min}^\mathrm{PC}$ from the others; here Euclidean distance is used.

5.4 Decision making

Path-planning algorithm

The planning of a new route is implemented as a modified Dijkstra algorithm over the coarse-grained place cell graph, provided as connectivity matrix C. Its particularity is the use of a weighting $\widetilde{\mathbf{W}}$ of the nodes according to the neuromodulation map.

Algorithm 1 Modified Dijkstra algorithm

Require: Connectivity matrix $\mathbf{C} \in \{0,1\}^{\mathrm{N^{PC}} \times \mathrm{N^{PC}}}$, Node coordinates $\mathbf{x} \in \mathbb{R}^{\mathrm{N^{PC}} \times 2}$, Node weights $\widetilde{\mathbf{W}} \in \mathbb{R}^{\mathrm{N^{PC}}}$, Start node s, End node t
Ensure: Shortest path from t_0 to T

distances $\leftarrow [\infty, \infty, \ldots, \infty]$ ▷ Initialize distances
distances[t_0] $\leftarrow 0$
parent $\leftarrow [-1, -1, \ldots, -1]$ ▷ Parent pointers
finalized $\leftarrow$ [false, false, ..., false] ▷ Set of finalized nodes
PQ $\leftarrow \emptyset$ ▷ Priority queue
PQ.push($(0, \mathrm{t}_0)$) ▷ Insert start node with priority 0
while PQ $\neq \emptyset$ **do**
    (dist, j) $\leftarrow$ PQ.extractMin()
    if finalized[j] or dist $>$ distances[j] **then**
        continue
    end if
    finalized[j] $\leftarrow$ true
    if j = T **then**
        break ▷ Destination reached
    end if
    for each node i where $\mathbf{C}_{\mathrm{i,j}} = 1$ and not finalized[i] **do**
        if $\widetilde{\mathbf{W}}$[i] < -1000 **then**
            continue ▷ Skip nodes with high negative weights
        end if
        $\Delta \mathrm{x} \leftarrow \mathbf{x}_{\mathrm{j},0} - \mathbf{x}_{\mathrm{i},0}$
        $\Delta \mathrm{y} \leftarrow \mathbf{x}_{\mathrm{j},1} - \mathbf{x}_{\mathrm{i},1}$
        edge_dist $\leftarrow \sqrt{\Delta \mathrm{x}^2 + \Delta \mathrm{y}^2}$ ▷ Euclidean distance
        new_dist $\leftarrow$ d[j] + edge_dist
        if new_dist $<$ d[i] **then**
            d[i] $\leftarrow$ new_dist
            parent[i] $\leftarrow$ u
            PQ.push((new_dist, i))
        end if
    end for
end while
path $\leftarrow$ []
if d[T] $= \infty$ **then**
    return $\emptyset$ ▷ No path exists
end if
curr $\leftarrow$ t
while curr $\neq -1$ **do**
    path.append(curr)
    curr $\leftarrow$ parent[curr]
end while
path.reverse()
if path is empty or path[0] $\neq$ s **then**
    return $\emptyset$
end if
return path